Plastic deformation and twinning mechanisms in magnesian calcites: a non-equilibrium computer simulation study

Sanha Lee,*‡ Gøran Brekke Svaland,*‡ and Fernando Bresme*

Department of Chemistry, Imperial College London, SW7 2AZ, United Kingdom
E-mail: g.svaland15@imperial.ac.uk, f.bresme@imperial.ac.uk
‡ *These authors contributed equally to this work*

Abstract

Deformation twinning provides a mechanism for energy dissipation in crystalline structures, with important implications on the mechanical response of carbonate biogenic materials. Carbonate crystals can incorporate magnesium, *e.g.* in the sea, modifying their elastic response significantly. We present a full atom computational investigation of the dependence of the twinning response of calcite with magnesium content, covering compositions compatible with three main structures, calcite, dolomite and magnesite. We find, in agreement with experiments that the incorporation of magnesium disfavors twinning as a dissipation mechanism in ordered structures (dolomite, magnesite), however the response is strongly dependent on the arrangement of the magnesium ions in the crystal structure. We show that structures with a high content of magnesium ($> 33\,\%$) in a disordered arrangement, lead to plastic response before twinning or fracturing. We demonstrate that the position of the magnesium ions plays a key role in the determination of the crystal deformation mode. This observation is correlated with the formation of percolation clusters of magnesium in magnesian calcites.

Introduction

In 1867 Friederich Eduard Reusch [15] understood that the reflecting planes observed in 1678 by Christian Huygens in Iceland spar calcite were the result of twin gliding in the crystal due to shear deformation. A star-like pattern could be seen around the point of impact where the crystal had been loaded by a sharp blow from a knife. Comparably, when the crystal were gradually loaded by a blunt tool, a pattern of similar character was observed. Deformation twinning can be an elastic or plastic deformation where the orientation of molecules in the crystal is changed systematically due to shear stress. Pressure twinning of calcite can be seen when slicing the crystal with a sharp blade across the edge of the cleavage plane [1]. There are four known twin planes in calcite [13]; $c = \{001\}$, $e = \{018\}$, $f = \{012\}$ and $r = \{104\}$.

Biological exoskeletons produced by various organisms such as corals, molluscs, crustaceans, formanifera and sea urchins are very hard materials that dissipate applied stresses effectively through mechanisms such as deformation twinning [10] and the presence of biogenic impurities such as proteins that are incorporated into the crystal lattice promoting its elasticity [3,8,13]. Furthermore, uniform incorporation of magnesium has been found to linearly increase the stiffness of the material [5,20] and hence improve its hardness and wearability. The ability of crystals to undergo twinning is an important factor to stop crack propagation [10]. Hence, microscopic investigations leading to an explanation of the the microscopic mechanism determining the twinning response of calcium/magnesium carbonate minerals is very important. To our knowledge there are no systematic studies that address this issue in a wide range of magnesium compositions. High magnesian content calcites (HMCC) incorporate more than 4 mol % of $MgCO_3$ [6], and feature the same structure of calcite. Magnesian calcites are in general metastable in marine environments, while HMCC are readily found in a wide range of compositions (4 to 40) mol % $MgCO_3$ in biogenic skeletons and abiotically precipitated carbonate sediments [6].

Côté et al. [3] explored recently the elastic properties of pure calcite and calcite with one random configuration of 5 and 10 mol % Mg^{2+}, incorporated into the crystal lattice. Côté et al. [3] argued that the impurities acts as deformation twinning nucleation points, due to increased local stresses and would therefore be advantageous in enhancing the deformation twinning of calcite.

Interestingly, magnesite, which is a crystal in the same space group as calcite where all the calcium ions are replaced by magnesium, does not display deformation twinning. On the other hand, dolomite, where half of the calcite Ca^{2+} lattice sites are occupied by Mg^{2+} ions in alternating layers along the c-axis, is known to deform by twinning as its principal mode of deformation along with slip on the c and f planes. However, twinning in dolomite happens at temperatures in the range 600-900 K [1,9], unlike calcite, where twinning is readily observed at 300 K. Indeed, dolomite features shear fracture as the principal mode of deformation at 300 K [9].

In this paper, we investigate using non-equilibrium uniaxial strain simulations, the impact that the incorporation of magnesium ions has on the elastic properties of calcite. We cover the whole range of compositions, from calcite (C) to magnesite (M) passing through dolomite (D), and inspect different magnesium arrangements, namely, the ones defining the C, M and D minerals, and random distribution of magnesium inside the crystals. The comparison of these different structures reveals large differences in the deformation modes of magnesian calcite under stress, which can be correlated with the distribution of the magnesium cation in the crystal structure.

Methods

The calcite, magnesite and dolomite unit cells were created from primitive cells downloaded from the American Mineralogist Database [4,11,18]. Molecular dynamics simulations were performed with LAMMPS [12]. We have used the force field parameters given by Tomono et al. [19]. The parameters of this force field for Mg^{2+} were fitted and added to the original rigid ion force field developed by Raiteri et al. [14]. The Raiteri force field was fitted to reproduce structural and mechanical properties of calcite and aragonite, as well as the free energy difference between these two crystal phases. Hence, the force field parameters given by Tomono et al. [19] represent a good starting point for our investigation.

The crystallographic c-axis corresponds to the z-axis in our simulations. The conventional or-

thorhombic unit cell was multiplied to generate $7 \times 5 \times 2$ periodic super-cells containing 420 $(Mg_x,Ca_{1-x})CO_3$ units. The choice of different supercells were found to give similar results (see Figures 16 and 17 in the Supplementary Information). The potential cutoff was set to 12.5 Å and long range coulombic interactions were handled using the PPPM Ewald summation method [7]. The time step used in the simulations was set to 2 fs and the temperature to 300 K, using the Nosé-Hoover thermostat and a relaxation time of 100 fs. The crystals were initially equilibrated for 100 ps in the NPT ensemble using the Nosé-Hoover barostat and a relaxation time of 500 fs. In order to investigate the impact of Mg^{2+} ions on the elastic properties, we introduced Mg^{2+} in the crystals by randomly replacing the Ca^{2+} ions at set compositions. Seven different ratios of magnesium:calcium (m:c) incorporation were investigated at (m:c) ratios of (0:6), (1:5), (2:4), (3:3), (4:2), (5:1) and (6:0) according to the formula,

$$Ca_cMg_m(CO_3)_{c+m} \tag{1}$$

The generated supercells containing Mg^{2+} ions were equilibrated for a further 100 ps before the stretching process. All stress components were equilibrated to 0 atm using the Nosé-Hoover barostat. The pressure was maintained via this barostat during the stretching process in all directions except the one corresponding to the applied strain. The supercell was stretched along the z-axis in small incremental steps reaching up to 30-35 % total strain for six different strain rates, s= (0.15, 0.20, 0.25, 0.30, 0.40 and 1.00) s^{-1}. The strain was computed from $\epsilon_z(t) = (L_{z,t} - L_{z,0})/L_{z,0}$, where $L_{z,t}$ is the box size in z at time t and $L_{z,0}$ the box length of the unstressed equilibrium configuration. The z-component of the stress was sampled every 5 ps, and the coordinates of the atoms were dumped every 10 ps. These atomic trajectories were used to study the twinning during the deformation of the bulk crystals. For the magnesian calcites with random Mg^{2+} distribution, we performed simulations using four different configurations for each composition. These configurations were generated using different random seeds.

For anisotropic materials such as calcite, magnesite and dolomite, the relation between stress and strain is given by eq. (2)

$$\sigma_{ij} = C_{ijkl}\epsilon_{kl} \tag{2}$$

where C_{ijkl} is the elastic/stiffness matrix and ϵ_{kl} the applied strain. The Young's modulus will depend on the direction of the applied strain. However, when uniaxial strain is applied in ij direction, and the stress σ_{ij}, in all the other directions is relaxed, the elastic matrix, C_{ijkl}, reduces to a coefficient E_{ij}, that can be quantified from the slope of the σ *vs.* ϵ graph, in the elastic regime:

$$\sigma_z = E_z\epsilon_z \tag{3}$$

where $\sigma_z = \sigma_{zz}$, and $\epsilon_z = \epsilon_{zz}$, are the stress and strain along the crystallographic c-axis, investigated in this paper.

Voronoi tessellation of Mg^{2+} and Ca^{2+} ions in the crystals were carried out using Voro^{++} [16], which were used to list neighboring particles depending on whether their Voronoi cells share a face. The resulting clusters were used to determine the percolation of magnesium ions in the crystals.

Results and discussion

We show in fig. 1 two examples of the structures resulting from the stretching process for crystals with the same Mg:Ca ratio, but using different initial configurations and different arrangements of Mg^{2+} ions. One final box geometry, T, features rows of carbonates pointing preferentially in the same direction along the b-axis, whereas for the final box geometry A, the orientations of the carbonate anions are alternating between pointing up and down along both a and b-vectors (periodic boundary conditions must be taken into consideration). Both final structures display similar ion-ion radial distribution functions but different volumes. The final volume of A type deformation is 60 % larger than the initial cell volume, whereas for the T type deformation the volume is 84 % larger than the initial cell (see figure 12 in the Supplementary Information). These results show the diversity in the final structures that can be obtained from the twinning process. In both cases we observed the same type of twinning, namely the r-type: {104} twin plane. In both cases, A and T, the carbonate molecules rotate around their center of mass, and the twin

plane of the rotated carbonates lies approximately 90° with respect to the untwinned carbonates. This structure propagates throughout the crystal until all the carbonates have rotated. The final configuration consists of rows of carbonates where the orientation of the oxygens (pointing up or down) in the carbonate alternate (A) along the a and b-axis, and alternate up and down in rows along the a-axis (T).

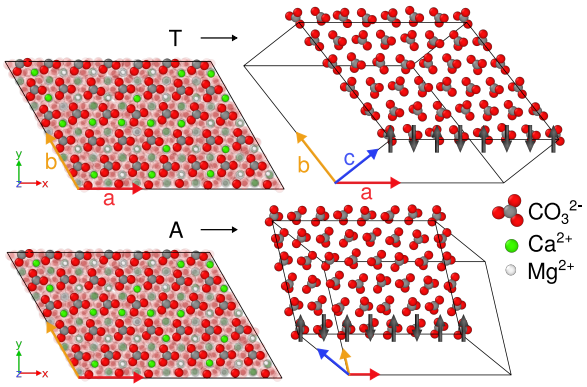

Figure 1: Deformation twinning type T and A shear deformation of the bulk system before (left) and after (right) 30 % applied strain along z-axis. Only carbonates in the first layer are shown for the final states (right). The arrows illustrate the preferred orientations of the carbonates along the a-axis.

In fig. 2 we show the stress component $\sigma_z(\epsilon_z)$ for the different Mg^{2+} concentrations. In the initial part of the strain process the crystal features an elastic response, with the stress component increasing linearly with strain. The blue line with the smallest slope corresponds to pure calcite and shows a very abrupt stress release at $\sim$ 10 GPa. The abrupt stress release is a characteristic feature of the pure crystals, including dolomite. The stress release reported in fig. 3a for calcite is a result of twinning. The elastic coefficient we obtain from our simulations, $E_z = 54$ GPa is comparable to other previous compuational estimates[3,17]. Incorporation of Mg^{2+} ions in the crystal leads to stress being released at approximately 2 % lower level of strain. In the case of magnesite, the stress builds up until the crystal fractures in a direction perpendicular to the direction of the applied strain. We observe the same fracture response in dolomite. Our simulations shows that dolomite endures a higher strain before fracturing, as compared with other crystals (see fig. 3). The elastic coefficient of the c-axis (E_z) for the different magnesian calcites was computed from the slope of the stress/strain curve before the crystal twins or fractures. We show in fig. 2 the elastic coefficient plotted as a function of Mg^{2+} content. Our model confirms the stiffening of magnesian calcite with increased Mg^{2+} concentration, a result consistent with previous observations[20]. We also find that the elastic coefficients for different strain rates fall on the same curve, indicating that our simulations are performed in the linear regime.

In fig. 3 we show snapshots of the crystals at different stress-strain configurations. Compared to all the magnesian calcites, pure calcite (fig. 3a) displays a very ordered transition from its initial phase to a twinned phase. For calcite, two twin planes are created at the first drop in σ_z (see fig. 3a). The twin planes span the whole crystal, and propagate perpendicular to the twin plane until the entire crystal is twinned. When some Mg^{2+} is incorporated randomly into the calcite lattice, we observe multiple twin planes throughout the crystal, which occurs at different levels of strain (se figs. 3b and 3c). This is probably due to lattice distortions as pointed out by Côté et al.[3], where locations of magnesium in the lattice introduces a higher local stress due to the smaller size of the Mg^{2+} ion as compared to Ca^{2+}. In addition, the complete twinning of the magnesian crystal occurs typically at higher levels of strain, (about 2 %) higher than the strain of pure calcite. The process of twinning the magnesian calcites occurs in several steps, as illustrated by the stress-strain curves in figs. 3a to 3c. This behavior is not observed in magnesite (fig. 3d) and dolomite. These crystals fracture in the direction perpendicular to the strain direction. While calcite yields by deformation twinning at 17 % strain, magnesite and dolomite yields by extension fracture at about 18 and 22 %, respectively. We also find that the stress-strain curve for magnesian calcites, all the way from the 2:4 to 5:1 Mg:Ca ratio display a plastic response close to their yield. The plastic response is characterized by a gradual decrease of the stress upon reaching the maximum stress, instead of a sudden drop. However the simulations show that this plastic response is not observed at low Mg^{2+} content, *e.g.* 1:5 Mg:Ca ratio (see figs. 2 and 3a), which releases the internal

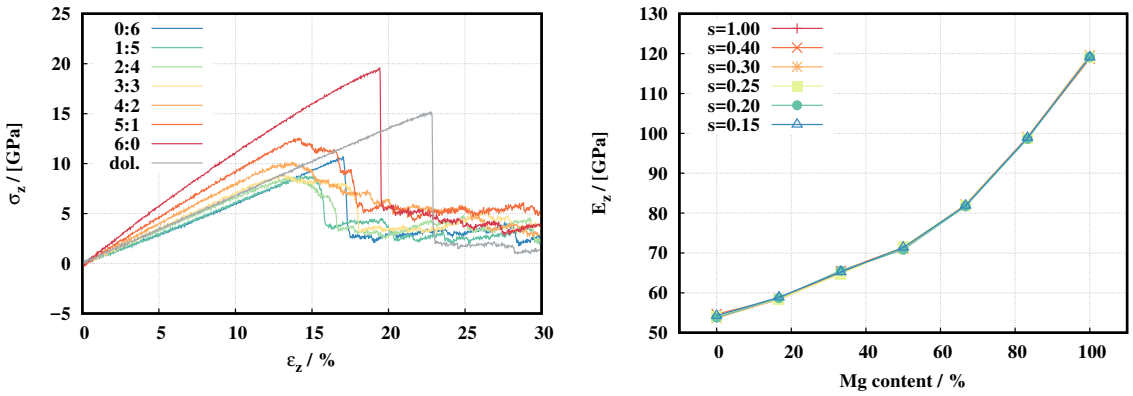

Figure 2: (Left) Stress as a function of strain rate for different Mg^{2+} concentrations and for dolomite (dol.). The strain was applied along the (001) plane. (Right) Dependence of the elastic coefficient E_z with Mg^{2+} content and for different strain rates. The largest standard error is ∼1.1 GPa.

stresses abruptly by deformation twinning, as observes in pure calcite. We looked into the possible origin of this distinctive deformation response for low and high Mg^{2+} contents by investigating the percolation threshold for the clusters of Mg^{2+} ions in the lattice. We found that the magnesium ions percolate, namely, they form an infinite cluster at 33 mol % $MgCO_3$ while they do not at the 1:5 Mg:Ca ratio (see figures 7, 6 and 9 in the Supplementary Information). We expect that the percolation threshold of Mg^{2+} must therefore be somewhere in the range of (16 to 33) mol % $MgCO_3$. The 3:3 composition, which also contains a percolating Mg^{2+} cluster, shows a much smoother transition (see fig. 3c) into the fully twinned mode at about 30 % strain, which contrasts with the abrupt stress release observed at lower compositions of magnesian calcites, or dolomite.

We show in table 1, a summary of the preferred response deformation mode of magnesian calcites in terms of fractures and twin deformations. The probability of observing a particular deformation mode $\alpha = \{T, A, F\}$ is $\bar{p}_\alpha = \frac{1}{N_c}\sum_{j=1}^{N_c} p_{\alpha,j}$, where $N_c = 24$ is the number of configurations sampled and $\delta_{\alpha,j}$ is 1 if the deformation mode of configuration j is α. Note that $\sum_\alpha \bar{p}_\alpha = 1$. The standard deviation for the probabilities was estimated from the analysis of $N_i = 6$ independent subaverages obtained from the N_c sample, such that the variance $\sigma^2_{\bar{p}_\alpha} = \frac{1}{N_i - 1}\sum_{i=1}^{N_i}(p_{\alpha,i} - \bar{p}_\alpha)^2$. The occurrence of twinning (T), alternate twinning (A) and fracture (F) type deformation displays a clear trend where F is observed for magnesite, dolomite and magnesian calcites when the Mg:Ca ratio is more than 50 %. Twinning (T) is the main type of deformation from uniaxial strain along the c-axis for magnesian calcites where less than 50 % of the Ca^{2+} lattice points are occupied by Mg^{2+}. The A type deformation twinning was only observed in 2 % of the cases, and only for the 2:4 and 3:3 Mg:Ca ratios.

Table 1: Probability of deformation twinning (T), alternate twinning (A) and shear fracture (F) during applied uniaxial strain along c-axis in magnesian calcites. The data were obtained from four independent simulations at each of the six strain rates: (0.15, 0.2, 0.25, 0.3, 0.4 and 1.0) s^{-1}. For the pure cases, calcite, magnesite and dolomite, data were obtained from one trajectory for each strain rate. $\sigma_{T,A,F}$ is the standard deviation of T,A and F respectively. All values in %.

Mg:Ca	T	σ_T	A	σ_A	F	σ_F
0:6	100	0	0	0	0	0
1:5	100	0	0	0	0	0
2:4	96	10	4	10	0	0
3:3	88	14	8	13	4	10
4:2	50	22	0	0	50	22
5:1	21	10	0	0	79	10
6:0	0	0	0	0	100	0
dolomite	0	0	0	0	100	0

Our simulations indicate the existence of two dif-

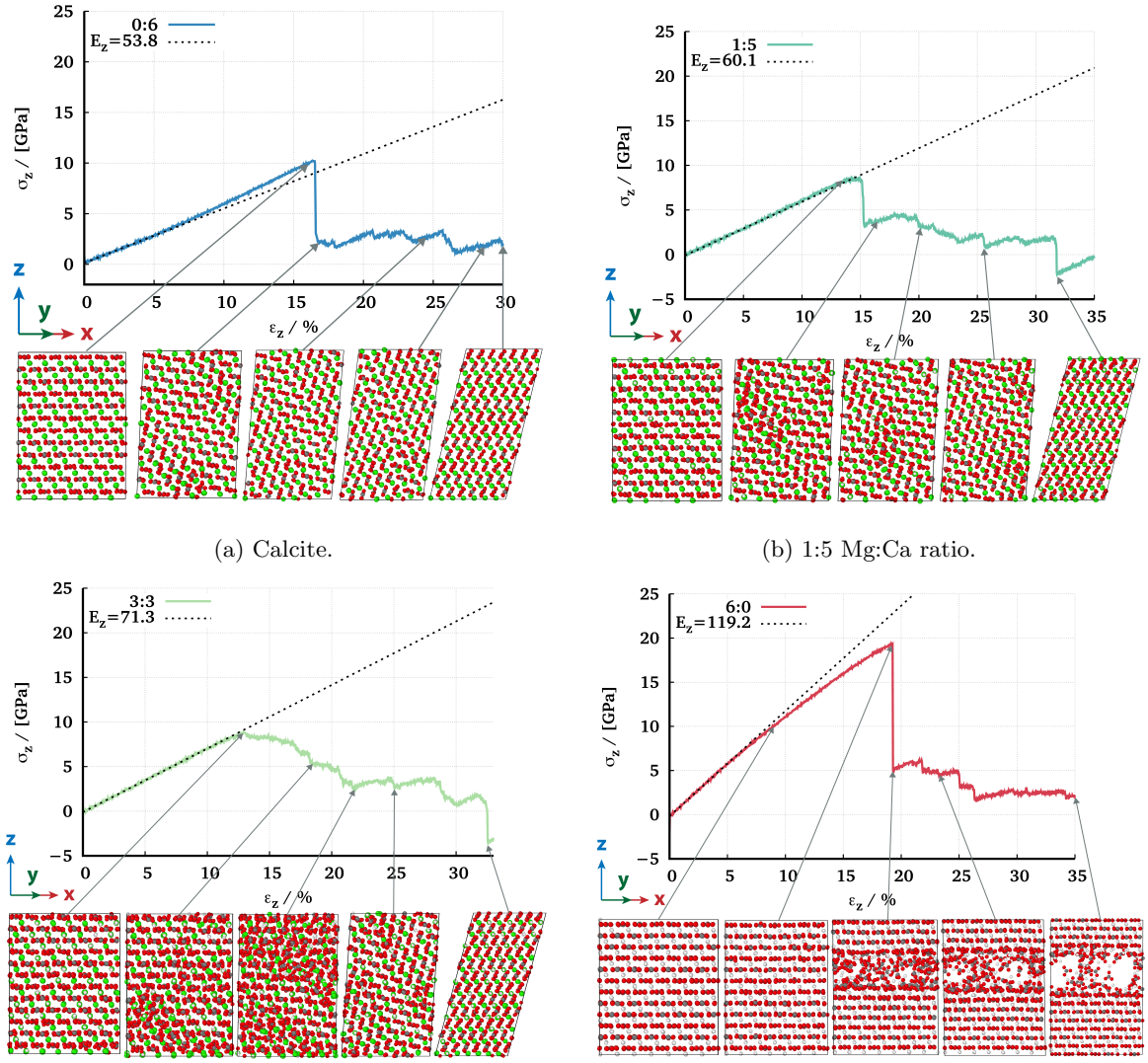

(a) Calcite.

(b) 1:5 Mg:Ca ratio.

(c) 3:3 Mg:Ca ratio.

(d) Magnesite.

Figure 3: Crystal deformation during applied strain along the z-axis. Snapshots of the crystal structure at different levels of strain is shown and indicated with arrows in the respective graphs.

ferent forms of shear deformation (T and A) for magnesian calcites with Mg:Ca ratios of 33 and 84 %. The shear deformation of the box is a result of the energetically favorable rotation of the carbonates when the crystal is under tension. Type T deformation is observed for all systems except for magnesite and dolomite, which always deform by fracture at 300 K. For both A and T type deformation, the {104} twin plane is the only observed deformation twinning that propagates through the crystal. The A type deformation however contributes very little to the deformation mode with a maximum of 8 % probability for 3:3 compositions (see Table 1).

As the concentration of magnesium in the calcite is increased, the mineral becomes harder and stiffer (fig. 2), and as we approach the 4:2 ratio of 67 mol % $MgCO_3$, there is a 50-50 chance of the

crystal deforming by fracture or deformation twinning at 300 K. From our data, the 50 % Mg:Ca ratio appears to be an important transition where we start to witness fracturing in most of the cases above 50 %, and twinning being the clearly favored deformation below. It is interesting to see that dolomite, which is a well-defined ordered crystal structure at 3:3 Mg:Ca ratio, fractures in all of the cases investigated here. Deformation twinning of dolomite has been shown experimentally,[1] but being a crystal of lower symmetry than calcite, it has fewer twin planes and r is not one of them. However, from compression of the c-axis, dolomite has been shown to deform by f type twinning[1]. But twinning only becomes an important mode of deformation in the experimental temperature range 600-900 K[1,2,9]. At lower temperatures, fracturing becomes a significant deformation mechanism for dolomite[2,9], and our results are consistent with this observation.

Conclusions

We have performed a systematic analysis of the deformation mode of magnesian calcites, pure calcite, dolomite and magnesite, by using non-equilibrium simulations by subjecting the crystal to uniaxial strain along the c-axis. Our analysis of magnesian calcites covers a wide range of compositions (16, 33, 50, 66 and 84) mol %, and addresses the impact that the arrangement of Mg^{2+} ions has on the stress relaxation mode. We conclude the following from our investigation:

• Magnesian calcites with compositions below 50 % Mg:Ca ratio deform under stress preferentially by deformation twinning, whereas at higher magnesium concentrations the crystal fractures.

• The dissipation mechanism of magnesian calcites depends both on the magnesium content and the arrangement of the magnesium ions in the lattice. Random insertion at low magnesium content (< 33 mol % $MgCO_3$) results in deformation twinning with a sharp decrease in the shear stress. At higher magnesium content, above 33 mol % $MgCO_3$, the magnesian calcites display instead a plastic behavior before yield or twinning. We found that at these higher compositions the magnesium ions form a percolating network that facilitates the dissipation via the plastic response unlike what is observed in ordered crystalline structures, *e.g.* dolomite.

• Calcites with less than 50 % Mg:Ca ratio feature stress dissipation through deformation twinning at approximately 2 % lower strain rates than that of pure calcite, and the energy dissipation continues for about 2 % more strain than for the pure calcite. This result indicates that on one hand, the material becomes more brittle as the concentration of magnesium is increased, but the incorporation of magnesium shifts at the same time the yield of the material to lower strain rates.

Overall, our work highlights the importance of both composition and microscopic ion distributions in determining the elastic response of biogenic minerals. In this paper we have restricted ourselves to deformation induced by applied strain, and not during compression, which is the most common experimental approach to generate stress. Increasing the pressure of the crystal along a crystallographic axis would be interesting and a possible next step for future computational studies.

Conflicts of interest

There are no conflicts of interest to declare.

Acknowledgement

This project is part of the NanoHeal network, and has received funding from the European Union's Horizon 2020 research and innovation programme under grant agreement No 642976. The computations reported in this work were performed in the Imperial College High Performance Computing Service.

References

[1] D. J. Barber and H. R. Wenk. Deformation twinning in calcite, dolomite, and other rhombohedral carbonates. *Phys. Chem. Min.*, 5(2):141–165, 1979. ISSN 14322021. doi: 10.1007/BF00307550.

[2] D. J. Barber, H. C. Heard, and H. R. Wenk. Deformation of dolomite single crystals from 20-800 C. *Phys. Chem.*

Min., 7(6):271–286, dec 1981. ISSN 0342-1791. doi: 10.1007/BF00311980. URL http://link.springer.com/10.1007/BF00311980.

[3] A. S. Côté, R. Darkins, and D. M. Duffy. Deformation twinning and the role of amino acids and magnesium in calcite hardness from molecular simulation. *Phys. Chem. Chem. Phys.*, 17(31):20178–20184, 2015. ISSN 1463-9076. doi: 10.1039/C5CP03370E. URL http://xlink.rsc.org/?DOI=C5CP03370E.

[4] Robert T. Downs and Michelle Hall-Wallace. The American Mineralogist crystal structure database. *American Mineralogist*, 88(1):247–250, 2003. ISSN 0003004X.

[5] Pavlína Elstnerová, Martin Friák, Helge Otto Fabritius, Liverios Lymperakis, Tilmann Hickel, Michal Petrov, Svetoslav Nikolov, Dierk Raabe, Andreas Ziegler, Sabine Hild, and Jörg Neugebauer. Ab initio study of thermodynamic, structural, and elastic properties of Mg-substituted crystalline calcite. *Acta Biomaterialia*, 6(12):4506–4512, 2010. ISSN 17427061. doi: 10.1016/j.actbio.2010.07.015.

[6] Jay M. Gregg, David L. Bish, Stephen E. Kaczmarek, and Hans G. Machel. Mineralogy, nucleation and growth of dolomite in the laboratory and sedimentary environment: A review. *Sedimentology*, 62(6):1749–1769, oct 2015. ISSN 00370746. doi: 10.1111/sed.12202.

[7] R. W. Hockney and J. W. Eastwood. *Computer simulation using particles*. CRC Press, 1989. ISBN 0852743920.

[8] Yi-Yeoun Kim, Kathirvel Ganesan, Pengcheng Yang, Alexander N. Kulak, Shirly Borukhin, Sasha Pechook, Luis Ribeiro, Roland Kröger, Stephen J. Eichhorn, Steven P. Armes, Boaz Pokroy, and Fiona C. Meldrum. An artificial biomineral formed by incorporation of copolymer micelles in calcite crystals. *Nat. Mat.*, 10 (11):890–896, sep 2011. ISSN 1476-1122. doi: 10.1038/nmat3103.

[9] Ann Kristin Larsson and Andrew G. Christy. On twinning and microstructures in calcite and dolomite. *American Mineralogist*, 93 (1):103–113, 2008. ISSN 0003004X. doi: 10.2138/am.2008.2520.

[10] Ling Li and Christine Ortiz. Pervasive nanoscale deformation twinning as a catalyst for efficient energy dissipation in a bioceramic armour. *Nat. mat.*, 13(5):501–7, 2014. ISSN 1476-1122. doi: 10.1038/nmat3920.

[11] S. A. Markgraf and R J Reeder. High-temperature structure refinements of calcite and magnesite. *Am. Mineral*, 70:590–600, 1985.

[12] Steve Plimpton. Fast Parallel Algorithms for Short-Range Molecular Dynamics. *J. Comp. Phys.*, 117(1):1–19, mar 1995. ISSN 00219991. doi: 10.1006/jcph.1995.1039.

[13] B. Pokroy, M. Kapon, F. Marin, N. Adir, and E. Zolotoyabko. Protein-induced, previously unidentified twin form of calcite. *PNAS*, 104 (18):7337–7341, 2007. ISSN 00278424. doi: 10.1073/pnas.0608584104.

[14] Paolo Raiteri, Julian D. Gale, David Quigley, and P. Mark Rodger. Derivation of an accurate force-field for simulating the growth of calcium carbonate from aqueous solution: A new model for the calcite-water interface. *J. Phys. Chem. C*, 114(13):5997–6010, 2010. ISSN 19327447. doi: 10.1021/jp910977a.

[15] E. Reusch. Ueber eine besondere gattung von durchgängen im steinsalz und kalkspath. *Annalen der Physik*, 208(11):441–451, 1867. ISSN 1521-3889. doi: 10.1002/andp.18672081106.

[16] Chris H. Rycroft. <scp>VORO++</scp> : A three-dimensional Voronoi cell library in C++. *Chaos: An Interdisciplinary Journal of Nonlinear Science*, 19(4):041111, dec 2009. ISSN 1054-1500. doi: 10.1063/1.3215722.

[17] W Sekkal and A Zaoui. Nanoscale analysis of the morphology and surface stability of calcium carbonate polymorphs. *Scientific reports*, 3:1587, 2013. ISSN 2045-2322. doi: 10.1038/srep01587.

[18] H Steinfink and F. J. Sans. REFINEMENT OF THE CRYSTAL STRUCTURE OF DOLOMITE. *The American Mineralogist*, 44:679–682, may 1959. ISSN 09090495.

[19] Hidekazu Tomono, Hiroki Nada, Fangjie Zhu, Takeshi Sakamoto, Tatsuya Nishimura, and Takashi Kato. Effects of Magnesium Ions and Water Molecules on the Structure of Amorphous Calcium Carbonate : A Molecular Dynamics Study. *J. Phys. Chem. B*, 117:14849–14856, 2013. ISSN 15206106. doi: 10.1021/jp407721x.

[20] L.-F. Zhu, M. Friák, L. Lymperakis, H. Titrian, U. Aydin, A.M. Janus, H.-O. Fabritius, A. Ziegler, S. Nikolov, P. Hemzalová, D. Raabe, and J. Neugebauer. Ab initio study of single-crystalline and polycrystalline elastic properties of Mg-substituted calcite crystals. *J. Mech. Behav. Biomed. Mater.*, 20: 296–304, apr 2013. ISSN 17516161. doi: 10.1016/j.jmbbm.2013.01.030.